

VIIRS Leaf Area Index (LAI) and Fraction of Photosynthetically Active Radiation Absorbed by Vegetation (FPAR) User Guide

Principal Investigator: Ranga B. Myneni
Correspondence e-mail address: rmyneni@bu.edu

Version 1.2
April 2018

This document was developed by Taejin Park, Kai Yan, Chi Chen, Baodong Xu,
Yuri Knyazikhin and Ranga Myneni

Department of Earth and Environment
Boston University

Change History Log

<i>Revision</i>	<i>Effective Date</i>	<i>Description of Changes</i>
V1.0	07/21/2017	First Draft has been prepared based on VNP15 V1.0 Development
V1.1	12/26/2017	Accuracy statement has been updated
V1.2	04/09/2018	Ancillary information in the product has been updated

This user's guide aims to present an overview of the new VIIRS Leaf Area Index (LAI) and Fraction of Photosynthetically Active Radiation Absorbed by Vegetation (FPAR) product (VNP15) to the potential user. The document describes the current state of the art, and is revised as progress is made in the development and assessment of the VIIRS LAI/FPAR product. For more details, please see the Algorithm Theoretical Basis Document (ATBD), posted in https://viirsland.gsfc.nasa.gov/PDF/VIIRS_LAI_ATBD_V1.0_19Jun2017.pdf.

Table of Content

1. Introduction	5
2. Definition	6
3. Algorithm Description	6
3.2.1 <i>VIIRS Sensor Specific LUTs</i>	7
3.2.2 <i>VIIRS Surface Reflectance (VNP09GA)</i>	8
3.2.3 <i>Global Land Cover Classification Map</i>	8
4. Standard VIIRS Product	9
5. Accuracy/Uncertainty Statement	16
6. Related Publications	18
7. How to Obtain the Data	18
8. Policies	18
9. Contact Information	18
10. Related Web Sites	19
11. References	19

Abbreviation

ATBD	Algorithm Theoretical Basis Documents
BRF	Bidirectional Reflectance Factor
C6	Collection 6
CDR	Climate Data Record
ECV	Essential Climate Variable
EOS	Earth Observing System
ESDR	Earth Science Data Record
ESDT	Earth Science Data Type
FPAR	Fraction of Photosynthetically Active Radiation
FTP	File Transfer Protocol
GCOS	Global Climate Observing System
HDF	Hierarchical Data Format
JPSS	Joint Polar Satellite System
L2G	Level 2 Gridded
LAI	Leaf Area Index
LC	Land Cover
LP DAAC	Land Process Distributed Active Archive Center
LUT	Look Up Table
MODIS	Moderate Resolution Imaging Spectroradiometer
NASA	National Aeronautics and Space Administration
NDVI	Normalized Difference Vegetation Index
NIR	Near Infra-Red
NPOESS	National Polar-orbiting Operational Environmental Satellite System
PGE	Product Generation Executable
QA	Quality Assurance
QC	Quality Control
RMSE	Root Mean Square Error
RT (RTM)	Radiative Transfer (Radiative Transfer Model)
SCF	Science Computing Facilities
SIN	Sinusoidal
SIPS	Science Investigator Processing System
SNPP	Suomi National Polar-orbiting Partnership
STD	Standard Deviation
V1	Version 1
VIIRS	Visible/Infrared Imager Radiometer Suite

1. Introduction

Both leaf area index (LAI) and fraction of photosynthetically active radiation (FPAR) that describe vegetation canopy structure and its energy absorption capacity are required by many of the Earth Observing System (EOS) Interdisciplinary Projects (Myneni et al., 1997). LAI/FPAR data thus has been acknowledged as a key Earth Science Data Record (ESDR) by the NASA Earth Science Division and an Essential Climate Variable (ECV) by the Global Climate Observing System (GCOS) (GCOS, 2006).

Efforts from the scientific community on developing global LAI/FPAR data using satellite observation have been made in last few decades (Knyazikhin et al., 1998; Myneni et al., 2002; Zhu et al., 2013; Baret et al., 2013). In particular, the groundbreaking EOS Moderate Resolution Imaging Spectroradiometer (MODIS) sensor onboard Terra and Aqua satellites provided an opportunity for opening a new horizon of global LAI/FPAR products (Myneni et al., 2002). A well-matured latest version (Collection 6, C6) of global LAI/FPAR data set (since February 2000) from this sensor is freely available and much in use by the wide scientific, public and private user communities (Yan et al., 2016a; Yan et al., 2016b).

The Visible/Infrared Imager Radiometer Suite (VIIRS) instrument onboard the Suomi National Polar-orbiting Partnership (SNPP) and Joint Polar Satellite System (JPSS) has inherited the scientific roles of MODIS (Justice et al., 2013). In this context, the NASA SNPP VIIRS LAI/FPAR product (VNP15) should ensure the continuity with the MODIS LAI/FPAR product (MxD15). Thus, transitioning of the MODIS algorithm to VIIRS is a high priority to continue the MODIS LAI/FPAR Earth Science Data Records (ESDRs). The overall objective for VIIRS Version 1 (V1) is to make the NASA VIIRS LAI/FPAR algorithms is compatible with the C6 MODIS Terra and Aqua LAI/FPAR algorithms to ensure continuity of the data products and enable development of a Climate Data Record (CDR) from the multi-sensors.

This document primarily aims to present an overview of the new VIIRS LAI/FPAR product (VNP15) to the potential user. The content includes (a) Overview of the algorithm, (b) Description of inputs and operational processing, (c) Description of the standard VNP15 product, and (d) Ways to obtain the product.

2. Definition

Leaf area index (LAI; dimensionless) is defined as the one-sided green leaf area per unit ground area in broadleaf canopies and as one-half the total needle surface area per unit ground area in coniferous canopies.

STD LAI is the estimated retrieval uncertainty, i.e., “true LAI” can differ from its retrieval counterpart by \pm STD (Standard Deviation) LAI (See [Figure 1](#)).

Fraction of Photosynthetically Active Radiation absorbed by vegetation (FPAR; dimensionless) is defined as the fraction of incident photosynthetically active radiation (400–700 nm) absorbed by the green elements of a vegetation canopy.

STD FPAR is the estimated retrieval uncertainty, i.e., “true FPAR” can differ from its retrieval counterpart by \pm STD FPAR (See [Figure 1](#)).

3. Algorithm Description

3.1. Overview of LAI/FPAR Algorithm

The VIIRS LAI/FPAR algorithm has benefitted from the heritage of the MODIS operational algorithm. The LAI/FPAR algorithm consists of a main Look-up-Table (LUT) based procedure that exploits the spectral information content of the VIIRS red (640 nm) and near-infrared (NIR, 865 nm) surface reflectances, and the back-up algorithm that uses empirical relationships between Normalized Difference Vegetation Index (NDVI) and canopy LAI and FPAR. The LUT was generated using 3D radiative transfer equation ([Knyazikhin et al., 1999](#)). Inputs to the algorithm are (i) vegetation structural type, (ii) sun-sensor geometry, (iii) BRFs at red and NIR spectral bands and (vi) their uncertainties. [Figure 1](#) illustrates the main algorithm: for each pixel it compares observed and modeled spectral Bidirectional Reflectance Factors (BRFs) for a suite of canopy structures and soil patterns that represent an expected range of typical conditions for a given biome type. All canopy/soil patterns and corresponding FPAR values for which modeled and observed BRFs differ within a specified uncertainty level are considered as acceptable solutions. The mean values of LAI, FPAR, their dispersions, STD LAI and STD FPAR, are reported as retrievals and their uncertainties ([Knyazikhin et al., 1999](#)). In the case of dense canopies, the reflectances saturate, and are therefore weakly sensitive to changes in canopy properties. The reliability of parameters retrieved under the condition of saturation is low, that is, the dispersion of the solution distribution is large. Such retrievals are flagged in QA layers ([Table 4](#)). When the LUT

method fails to localize a solution, the back-up method is utilized. The algorithm path (main or backup) is archived in QA layers (Table 4). Analyses of the algorithm performance indicate that best quality, high precision retrievals are obtained from the main algorithm (Yang et al. 2006). The algorithm path is therefore a key quality indicator.

The algorithm has interfaces with the VIIRS Surface Reflectance Product (VNP09GA) and the MODIS Land Cover Product. Technical details of the algorithm can be found in the Algorithm Theoretical Basis Document (ATBD,

https://viirsland.gsfc.nasa.gov/PDF/VIIRS_LAI_ATBD_V1.0_19Jun2017.pdf).

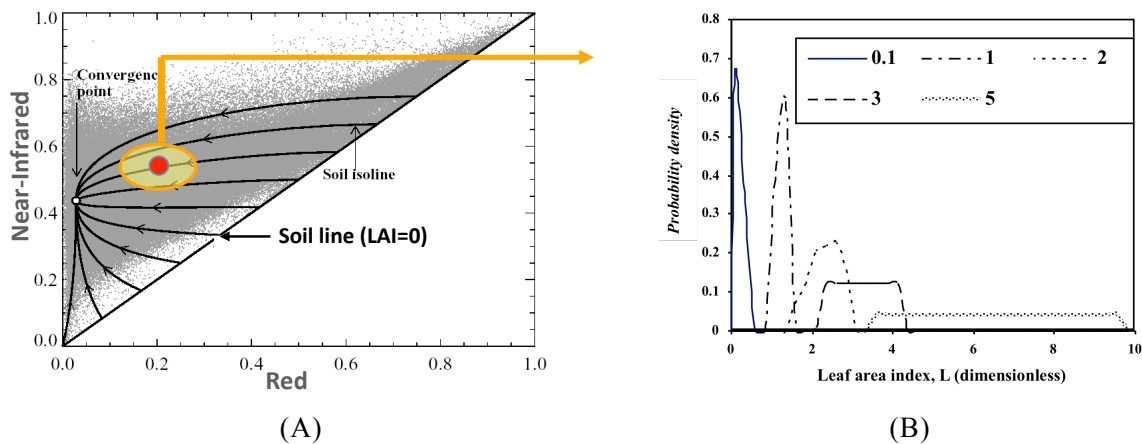


Figure 1. Schematic illustration of the main algorithm. (A) Distribution of vegetated pixels with respect to their reflectances at red and near-infrared (NIR) spectral bands. A point on the red-NIR plane and an area about it (yellow ellipse defined by a χ^2 distribution) are treated as the measured BRF at a given sun-sensor geometry and its uncertainty. Each combination of canopy/soil parameters and corresponding FPAR values for which modeled reflectances belong to the ellipse is an acceptable solution. (B) Density distribution function of acceptable solutions. Shown is solution density distribution function of LAI for five different pixels. The mean LAI and its dispersion (STD LAI) are taken as the LAI retrieval and its uncertainty. The figures are quoted from Knyazikhin et al. (1999).

3.2. Product Input

3.2.1 VIIRS Sensor Specific LUTs

The generation of consistent LAI/FPAR ESDRs from MODIS and VIIRS requires parameterizations that account for sensor-specific features - spatial resolution, bandwidth, calibration, atmospheric correction, information content, etc. Based on the theory of “canopy spectral invariants” (Knyazikhin et al., 1998; Huang et al., 2007; Knyazikhin et al., 2013), VIIRS-specific LUTs have been developed and incorporated.

The theoretical and technical details can be found in the VIIRS LAI/FPAR Algorithm Theoretical Basis Document (ATBD,

https://viirsland.gsfc.nasa.gov/PDF/VIIRS_LAI_ATBD_V1.0_19Jun2017.pdf).

3.2.2 VIIRS Surface Reflectance (VNP09GA)

The VIIRS Level 2G (L2G) surface reflectance product called VNP09GA (daily and 500 m) is used to generate daily LAI/FPAR product. Theoretically, the LAI/FPAR algorithm can make use of multiple atmosphere-corrected BRFs and their uncertainties (Wang et al., 2001). In practice, due to increasing uncertainty level by incorporating more spectral bands (Knyazikhin et al., 1999), the algorithm only uses red (640 nm) and NIR (865 nm) (i.e., I1 and I2) bands for the operational production. Details of VNP09GA can be found in Franch et al. (2016) and Roger et al. (2016) (see https://lpdaac.usgs.gov/dataset_discovery/viirs/viirs_products_table/vnp09ga).

3.2.3 Global Land Cover Classification Map

The algorithm chooses a strategy to run through all available vegetated pixels without masking or screening process (e.g., cloud, aerosol and cloud shadow mask etc.) rather than pre-masking inputs before algorithm implementation. This is beneficial to minimize the impact of upstream products. The only required ancillary data for the LAI/FPAR algorithm is the global 8-biome map. Introducing this biome map enables simplified assumptions and standardized constants (e.g., vegetation and soil optical properties) that vary with biome and soil types only. Thus, using the biome map as prior-knowledge can reduce the number of unknowns of the “ill-posed” inverse problem (Myneni et al., 2002). Note that current input global biome map for developing VIIRS LAI/FPAR algorithm and its production is supported from MODIS LC product (500 m) at this stage and will be updated with VIIRS data at a later date.

3.3. Production Logic and Data Flow

This section aims to briefly describe the data production logic and data flow scheme implemented in Land SIPS (Figure 2). VIIRS LAI/FPAR operational production separates two algorithm steps: a) daily LAI/FPAR algorithm (refers to PGE533) and b) 8-day compositing algorithm (refers to PGE534). Details of the production logic and data flow can be found in Section 3.3 of the VIIRS LAI/FPAR ATBD.

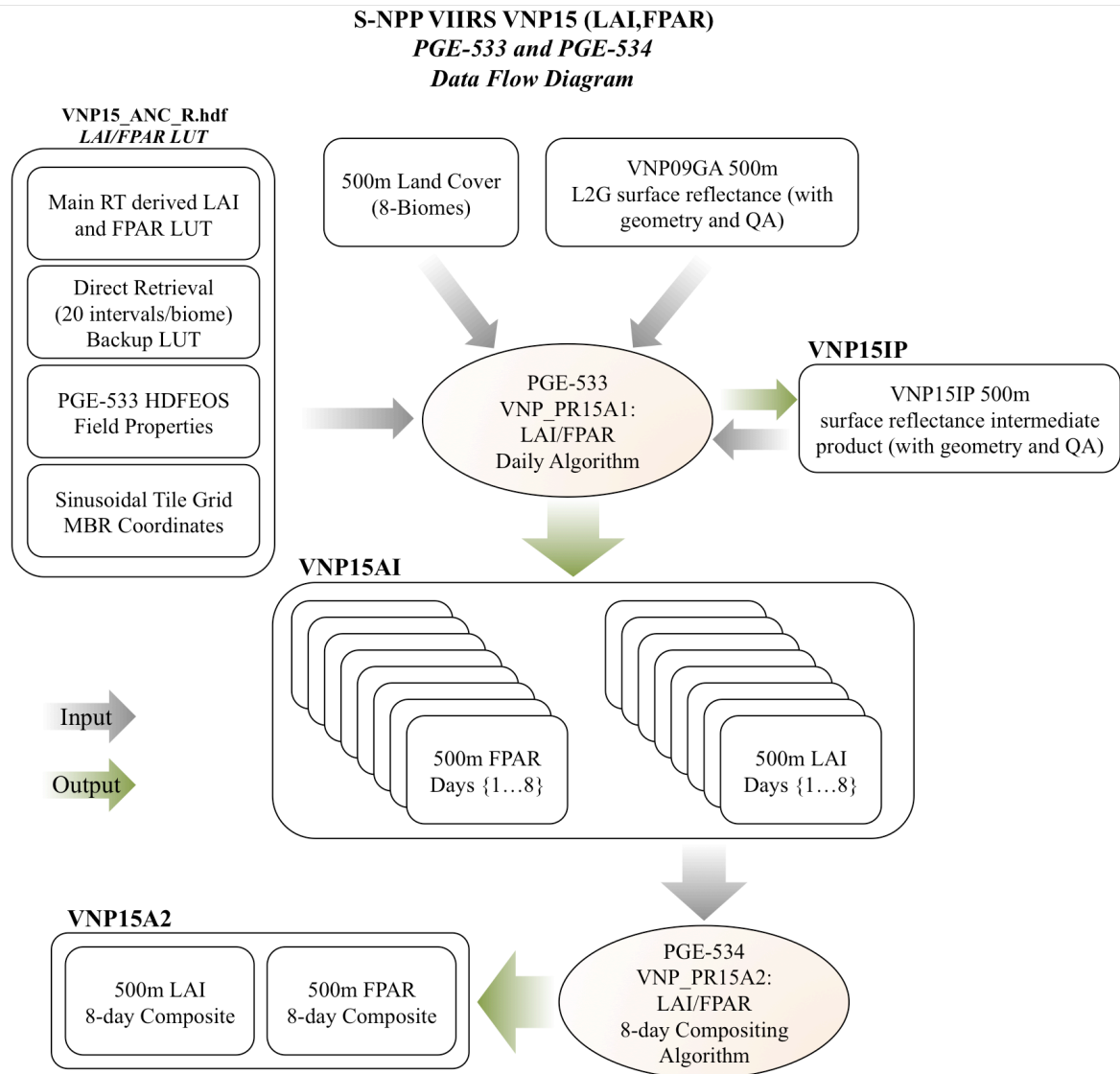


Figure 2. Algorithm flow of the operational VIIRS LAI/FPAR Version 1 production.

4. Standard VIIRS Product

The standard VIIRS V1 LAI/FPAR product (VNP15A2H) is at 500-meter spatial resolution based on 8-day temporal compositing approach (Table 1).

Table 1. LAI/FPAR products produced by Land SIPS

Product	ESDT	Raster Type	Spatial Resolution	Temporal Granularity
VIIRS LAI/FPAR	VNP15A2H*	Tile	500m	8-day

ESDT: Earth Science Data Type

*: Available via Land Process Distributed Active Archive Center (LP DAAC) (<https://lpdaac.usgs.gov>)

The VIIRS product uses the Sinusoidal grid tiling system (Figure 3) that is consistent with MODIS tiling system. Tiles are 10 degrees by 10 degrees at the equator (Table 2). The tile coordinate system starts at (0, 0) (horizontal tile number, vertical tile number) in the upper left corner and proceeds right (horizontal) and downward (vertical). The tile in the bottom right corner is (35, 17).

Table 2. Data set characteristics of the VIIRS LAI/FPAR product

Characteristics	V1 Product
Temporal Coverage	January 19, 2012 – Present
Spatial Extent	Global
Tile Coverage	~ 10° × 10° lat/long
File Size	~ 34.6 MB compressed
Projection	Sinusoidal
Data Format	HDF–EOS5
Dimensions	2400 × 2400 rows/columns (1200km × 1200km)
Resolution	500 meter
Science Data Sets (SDS HDF Layers)	6

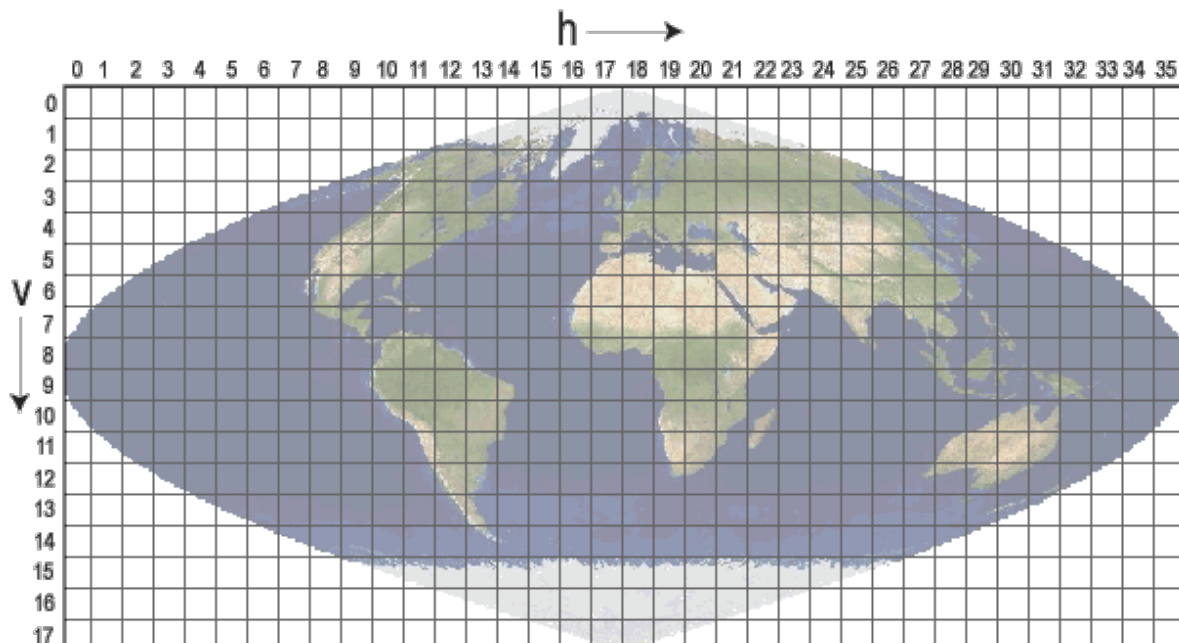


Figure 3. The Suomi-NPP VIIRS sinusoidal grid consists of 460 non-overlapping tiles which measure approximately 10° × 10° region. This sinusoidal grid projection and tiling scheme are exactly consistent with MODIS land products.

SNPP VIIRS LAI/FPAR data are provided in the standard land HDF-EOS5 format, which is beneficial to efficiently manage multidimensional arrays of NASA science records and structures for grouping objects. VIIRS product filenames (i.e., the local granule ID) follow a naming convention that gives useful information regarding the product. For example, the filename

VNP15A2H.A2015345.h28v05.001.2016292234657.h5 indicates:

- VNP15A2H – Product Short Name
- .A2015345 – Julian Date of Acquisition (A–YYYYDDD)
- .h28v05 – Tile Identifier (horizontal XX, vertical YY)
- .001 – Product Version
- .2016292234657 – Julian Date of Production (YYYYDDDDHHMMSS)
- .h5 – Data Format (HDF5)

VIIRS products have two sources of metadata: the embedded HDF-EOS5 metadata, and the external ECS metadata. The HDF-EOS5 metadata contains valuable information including global attributes and dataset specific attributes pertaining to the granule. An external metadata file is provided in XML format (.xml) and is provided along with the VIIRS product. This file provides a subset of the HDF-EOS5 metadata. Some key features of certain VIIRS HDF-EOS5 metadata attributes include the following:

- The *Xdim* and *Ydim* represent the rows and columns of the data, respectively.
- The *Projection* and *ProjParams* identify the projection and its corresponding projection parameters.
- The *Sinusoidal Projection* is used for most of the gridded VIIRS land products, and has a unique sphere measuring 6371007.181 meters.
- The *UpperLeftPointMtrs* is in projection coordinates, and identifies the very upper left corner of the upper left pixel of the image data.
- The *LowerRightMtrs* identifies the very lower right corner of the lower right pixel of the image data. These projection coordinates are the only metadata that accurately reflect the extreme corners of the gridded image.
- There are additional *BOUNDINGRECTANGLE* and *GRINGPOINT* fields within the metadata, which represent the latitude and longitude coordinates of

the geographic tile corresponding to the data.

4.1. Content of the product file

The VIIRS LAI/FPAR product is at 500-meter resolution in a Sinusoidal grid. Science Data Sets (SDSs) provided in the product include LAI, FPAR, quality ratings, and standard deviation for each variable, STD LAI and STD FPAR (Table 3).

Table 3. Scientific Data Sets included in the VIIRS LAI/FPAR product

Scientific Data Sets (HDF Layers) (6)	Units	Bit Type	Fill Value	Valid Range	Multiply By Scale Factor
Fpar	Dimensionless (Fraction)	8-bit unsigned integer	249–255	0–100	0.01
Lai [#]	Dimensionless (m ² plant/m ² ground)	8-bit unsigned integer	249–255	0–100	0.1
FparLai_QC	Class flag	8-bit unsigned integer	255	0–254	N/A
FparExtra_QC	Class flag	8-bit unsigned integer	255	0–254	N/A
FparStdDev	Dimensionless (Fraction)	8-bit unsigned integer	248–255	0–100	0.01
LaiStdDev [#]	Dimensionless (m ² plant/m ² ground)	8-bit unsigned integer	248–255	0–100	0.1

One-tile sample images illustrating how the VIIRS V1 VNP15A2H LAI, FPAR and STD-LAI spatial fields will look are shown below, for test file H20V08 (Central Africa) in the 10 degree Sinusoidal grid (Figure 4).

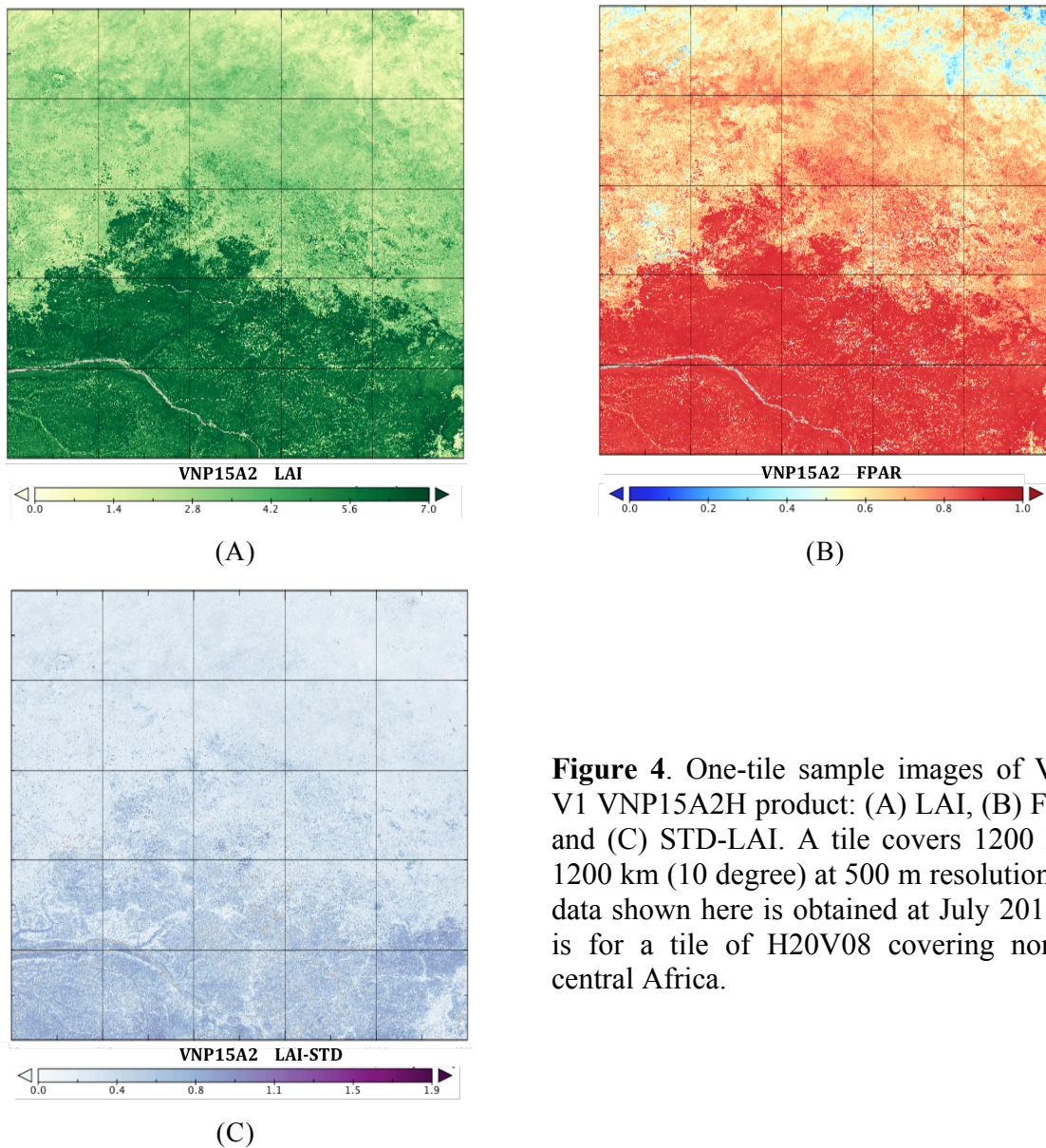


Figure 4. One-tile sample images of VIIRS V1 VNP15A2H product: (A) LAI, (B) FPAR, and (C) STD-LAI. A tile covers $1200 \text{ km} \times 1200 \text{ km}$ (10 degree) at 500 m resolution. The data shown here is obtained at July 2015 and is for a tile of H20V08 covering northern central Africa.

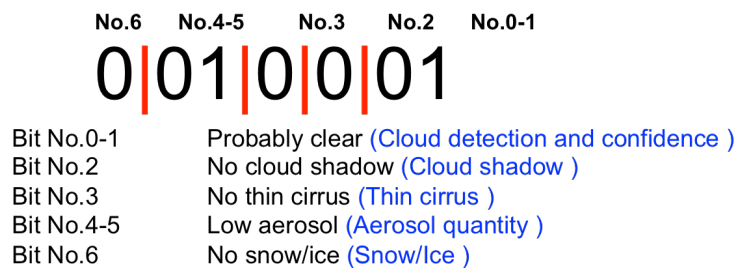
4.2. Description of QC SDS

Pixel-wise QC information of tiled VIIRS LAI/FPAR product is represented by two SDS layers (FparLai_QC and FparExtra_QC) (See [Table 3](#)). Note that the LAI/FPAR algorithm is executed irrespective of input quality. Therefore user should consult the QC layers of the LAI/FPAR product to select reliable retrievals. The key indicator of retrieval quality of the LAI/FPAR product is SCF_QC bit field in FparLai_QC SDS layer that represents algorithm path. Details of quality flags of the product are shown in following tables ([Table 4 and 5](#))

Table 5. Values of FparExtra_QC

Bit No.	Parameter Name	Bit Comb.	FparExtra_QC
0-1	Cloud detection and confidence	00	0 Confident clear
		01	1 Probably clear
		10	2 Probably cloudy
		11	3 Confident cloudy
2	Cloud shadow	0	0 No cloud shadow
		1	1 Shadow
3	Thin cirrus	0	0 No
		1	1 Yes
4-5	Aerosol quantity	00	0 Climatology
		01	1 Low
		10	2 Average
		11	3 High
6	Snow/Ice	0	0 No
		1	1 Yes

Example for interpretation of FparExtra_QC bit-strings is shown in [Figure 6](#). Please refer to [Table 5](#) for interpretation.

**Figure 6.** Example of FparExtra_QC bit-string and its interpretation

And fill value legends for SDS layers are given in [Table 6 and 7](#). Using the global LC product, each 500m pixel is classified according to its status as a land or non-land pixel. A number of non-terrestrial pixel classes are now carried through in the product data pixels (not QA/QC pixels) when the algorithm could not retrieve a biophysical estimate ([Table 6 and 7](#)).

Table 6. LAI and FPAR Fill value Legends

Value	Description
255	Fillvalue, assigned when: the VNP09GA surface reflectance for channel VIS, NIR was assigned as Fillvalue, or land cover pixel itself was assigned Fillvalue 255 or 254
254	land cover assigned as perennial salt or inland fresh water
253	land cover assigned as barren, sparse vegetation (rock, tundra, desert)
252	land cover assigned as perennial snow, ice
251	land cover assigned as “permanent” wetlands/inundated marshlands
250	land cover assigned as urban/built-up
249	land cover assigned as “unclassified” or not able to determine

Table 7. STD LAI and STD FPAR Fill Value Legends

Value	Description
255	Fillvalue, assigned when: the VNP09GA surface reflectance for channel VIS, NIR was assigned its Fillvalue, or land cover pixel itself was assigned Fillvalue 255 or 254
254	land cover assigned as perennial salt or inland fresh water
253	land cover assigned as barren, sparse vegetation (rock, tundra, desert)
252	land cover assigned as perennial snow, ice
251	land cover assigned as “permanent” wetlands/inundated marshlands
250	land cover assigned as urban/built-up
249	land cover assigned as “unclassified” or not able to determine
248	No standard deviation available, pixel produced using backup method

5. Accuracy/Uncertainty Statement

Validation at stage 1 has been achieved for the VIIRS V1 LAI/FPAR product. Related publications can be found in [Section 6](#).

Two validation efforts (i.e., direct and indirect) have been made for the statement of VIIRS LAI/FPAR Accuracy. The direct approach uses all available ground measured LAI/FPAR dataset ([Figure 7A-B](#)) and the indirect approach compares VIIRS LAI/FPAR retrievals to those of MODIS ([Figure 7C-D](#)). As the ground measurements obtained in VIIRS era are spatiotemporally limited, considering well-matured and -validated MODIS product as additional validation data source is justified.

For the direct approach, when all ground LAI measurements considering clumping effect are taken in account, the accuracy of LAI is 0.60 LAI unit RMSE ([Figure 7A](#)). The accuracy of FPAR is 0.10 FPAR unit RMSE ([Figure 7B](#)). The indirect approach indicates highly consistent LAI/FPAR retrievals from both VIIRS and MODIS during

first 5-year (2012-2016) of VIIRS era. Estimated mean differences between VIIRS and MODIS are less than 0.05 for LAI and 0.01 for FPAR. This result imbues the confidence that the VIIRS product is comparable with MODIS (MODIS Validation Stage: <https://landval.gsfc.nasa.gov/ProductStatus.php?ProductID=MOD15>, Yan et al., 2016b).

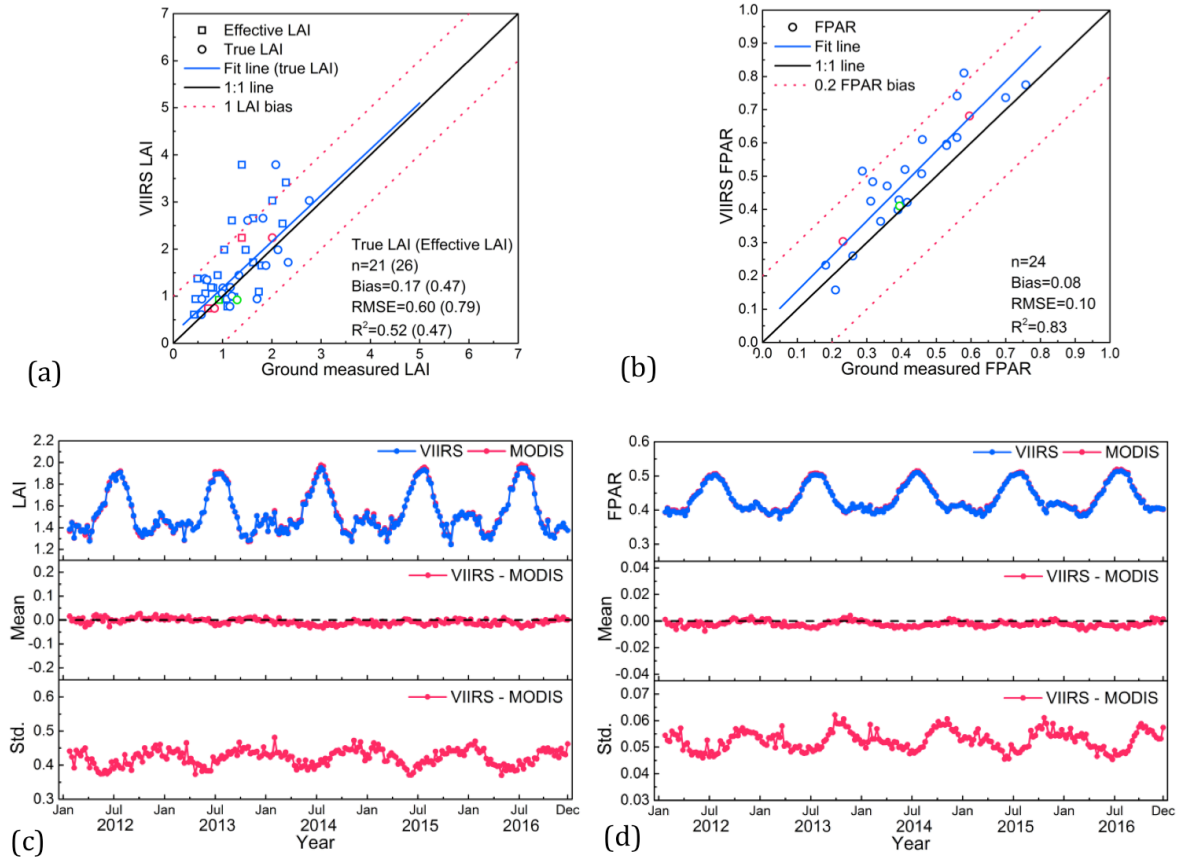


Figure 7. Comparison between VIIRS V1 and ground measured LAI/FPAR: (A) LAI and (B) FPAR. 21 true LAI, 26 effective LAI and 24 FPAR measurements are used here. The 3km \times 3km sites dominated by different biome types are depicted by different colors. Circles (squares) in LAI panel represent ground LAI measurements corrected (not corrected) for clumping. Comparison between global VIIRS V1 and MODIS C6 LAI/FPAR during 2012-2016: (C) LAI and (D) FPAR. The upper panel displays seasonal and annual variation of VIIRS and MODIS retrievals. Following middle (lower) panel shows seasonal and annual variation of mean difference (std. of difference) between VIIRS and MODIS.

The sites used in this validation practice are spatiotemporally limited to represent major global vegetation types and to cover different temporal periods. Thus, the product is considered to be validated to stage 1. All results presented here will be published in a peer-reviewing journal soon and the statement will be updated once the VIIRS validation activity has been additionally completed. Please check further information from following VIIRS Land Validation Status: https://viirsland.gsfc.nasa.gov/Val/LAI_Fpar_Val.html.

6. Related Publications

Yan, K., Park, T., Chen, C., Xu, B., Song, W., Yang, B., Zeng, Y., Liu, Z., Yan, G., Knyazikhin, Y. and Myneni, R.B., 2018. Generating Global Products of LAI and FPAR From SNPP-VIIRS Data: Theoretical Background and Implementation. IEEE Transactions on Geoscience and Remote Sensing.

Xu, B., Park, T., Yan, K., Chen, C., Zeng, Y., Song, W., Yin, G., Li, J., Liu, Q., Knyazikhin, Y. and Myneni, R.B., 2018. Analysis of Global LAI/FPAR Products from VIIRS and MODIS Sensors for Spatio-Temporal Consistency and Uncertainty from 2012–2016. Forests, 9(2), p.73.

7. How to Obtain the Data

The following tools offer options to search the LP DAAC data holdings and provide access to the data:

Bulk download: [LP DAAC Data Pool](#) and [DAAC2Disk](#)

Search and browse: [USGS EarthExplorer](#) and [NASA Earthdata Search](#)

Subset and explore: [AppEEARS](#)

8. Policies

Please find the current VIIRS–related Data policies on the VIIRS Policies page at https://lpdaac.usgs.gov/dataset_discovery/viirs/viirs_policies.

For information on how to cite LP DAAC data, please see our Data Citations page at https://lpdaac.usgs.gov/citing_our_data.

9. Contact Information

Ranga Myneni

Department of Geography and Environment, Boston University

Email: rmyneni@bu.edu

Web: <http://sites.bu.edu/cliveg>

10. Related Web Sites

- *Suomi-NPP*
<http://npp.gsfc.nasa.gov/suomi.html>
- *VIIRS*
VIIRS Land: <http://viirsland.gsfc.nasa.gov/>
VIIRS Land Product Quality Assessment:
https://landweb.nascom.nasa.gov/NPP_QA/
- *HDF5*
The HDF Group: <https://www.hdfgroup.org/HDF5/>
- *VIIRS/MODIS LAI/FPAR related Publications*
<http://sites.bu.edu/cliveg/research/vegetation-remote-sensing/>

11. References

- Baret, F., Weiss, M., Lacaze, R., Camacho, F., Makhmara, H., Pacholczyk, P. and Smets, B., 2013. GEOV1: LAI and FAPAR essential climate variables and FCOVER global time series capitalizing over existing products. Part1: Principles of development and production. *Remote Sensing of Environment*, 137, pp.299-309.
- Franch, B., Roger, J.C. and Vermote, E.F. 2016. Suomi-NPP VIIRS Surface Reflectance Algorithm Theoretical Basis Document (ATBD) – Version 2.0. viewed 1 March 2017, from https://viirsland.gsfc.nasa.gov/PDF/ATBD_VIIRS_SR_v2.pdf
- Global Climate Observing System (GCOS), Systematic observation requirements for satellitebased products for climate, GCOS-107, World Meteorol. Organ., Geneva, Switzerland, 2006.
- Huang, D., Knyazikhin, Y., Dickinson, R.E., Rautiainen, M., Stenberg, P., Disney, M., Lewis, P., Cescatti, A., Tian, Y., Verhoef, W. and Martonchik, J.V., 2007. Canopy spectral invariants for remote sensing and model applications. *Remote Sensing of Environment*, 106(1), pp.106-122.
- Justice, C.O., Román, M.O., Csizsar, I., Vermote, E.F., Wolfe, R.E., Hook, S.J., Friedl, M., Wang, Z., Schaaf, C.B., Miura, T. and Tschudi, M., 2013. Land and cryosphere products from Suomi NPP VIIRS: Overview and status. *Journal of Geophysical Research: Atmospheres*, 118(17), pp.9753-9765.
- Knyazikhin, Y., Martonchik, J.V., Myneni, R.B., Diner, D.J. and Running, S.W., 1998. Synergistic algorithm for estimating vegetation canopy leaf area index and fraction of absorbed photosynthetically active radiation from MODIS and MISR data. *Journal of Geophysical Research*, 103(D24), p.32257.
- Knyazikhin, Y., Glassy, J., Privette, J.L., Tian, Y., Lotsch, A., Zhang, Y., Wang, Y., Morisette, J.T., Votava, P., Myneni, R.B. and Nemani, R.R., 1999. MODIS leaf area index (LAI) and

fraction of photosynthetically active radiation absorbed by vegetation (FPAR) product (MOD15) algorithm theoretical basis document. Theoretical Basis Document, NASA Goddard Space Flight Center, Greenbelt, MD, 20771.

- Knyazikhin, Y., Schull, M.A., Stenberg, P., Mõttus, M., Rautiainen, M., Yang, Y., Marshak, A., Carmona, P.L., Kaufmann, R.K., Lewis, P. and Disney, M.I., 2013. Hyperspectral remote sensing of foliar nitrogen content. *Proceedings of the National Academy of Sciences*, 110(3), pp.E185-E192.
- Myneni, R.B., Ramakrishna, R., Nemani, R. and Running, S.W., 1997. Estimation of global leaf area index and absorbed PAR using radiative transfer models. *IEEE Transactions on Geoscience and remote sensing*, 35(6), pp.1380-1393.
- Myneni, R.B., Hoffman, S., Knyazikhin, Y., Privette, J.L., Glassy, J., Tian, Y., Wang, Y., Song, X., Zhang, Y., Smith, G.R. and Lotsch, A., 2002. Global products of vegetation leaf area and fraction absorbed PAR from year one of MODIS data. *Remote Sensing of Environment*, 83(1), pp.214-231.
- Roger, J.C., Vermote, E.F., Devadiga, S. and Ray, J.P. 2016. Suomi-NPP VIIRS Surface Reflectance User's Guide – Version 1. viewed 1 March 2017, from https://viirsland.gsfc.nasa.gov/PDF/VIIRS_Surf_Refl_UserGuide_v1.1.pdf
- Wang, Y., Tian, Y., Zhang, Y., El-Saleous, N., Knyazikhin, Y., Vermote, E. and Myneni, R.B., 2001. Investigation of product accuracy as a function of input and model uncertainties: Case study with SeaWiFS and MODIS LAI/FPAR algorithm. *Remote Sensing of Environment*, 78(3), pp.299-313.
- Yan, K., Park, T., Yan, G., Chen, C., Yang, B., Liu, Z., Nemani, R.R., Knyazikhin, Y. and Myneni, R.B., 2016a. Evaluation of MODIS LAI/FPAR product collection 6. Part 1: Consistency and improvements. *Remote Sensing*, 8(5), p.359.
- Yan, K., Park, T., Yan, G., Liu, Z., Yang, B., Chen, C., Nemani, R.R., Knyazikhin, Y. and Myneni, R.B., 2016b. Evaluation of MODIS LAI/FPAR Product Collection 6. Part 2: Validation and Intercomparison. *Remote Sensing*, 8(6), p.460.
- Yang, W., Shabanov, N.V., Huang, D., Wang, W., Dickinson, R.E., Nemani, R.R., Knyazikhin, Y. and Myneni, R.B., 2006. Analysis of leaf area index products from combination of MODIS Terra and Aqua data. *Remote Sensing of Environment*, 104(3), pp.297-312.
- Zhu, Z., Bi, J., Pan, Y., Ganguly, S., Anav, A., Xu, L., Samanta, A., Piao, S., Nemani, R.R. and Myneni, R.B., 2013. Global data sets of vegetation leaf area index (LAI) 3g and Fraction of Photosynthetically Active Radiation (FPAR) 3g derived from Global Inventory Modeling and Mapping Studies (GIMMS) Normalized Difference Vegetation Index (NDVI3g) for the period 1981 to 2011. *Remote Sensing*, 5(2), pp.927-948.